Materials Horizons

Optically addressable dielectric elastomer actuator arrays using embedded percolative networks of zinc oxide nanowires

Journal:	*Materials Horizons*
Manuscript ID	MH-COM-08-2022-001032.R1
Article Type:	Communication
Date Submitted by the Author:	27-Sep-2022
Complete List of Authors:	Hajiesmaili, Ehsan; Harvard University, School of Engineering and Applied Sciences Clarke, David; Harvard University, School of Engineering and Applied Sciences

New concepts:

One of the major challenges in creating shape changes using arrays of dielectric elastomer actuators (DEAs) is how to address and actuate individual actuators in an array since each actuator needs to be controlled separately. The challenge is compounded since the number of connections increases with the number of actuators in the array and the driving voltages are high. The new concept is to integrate stretchable photoconductive electrical channels, consisting of percolating networks of semiconducting nanowires, during the fabrication of the arrays, and use their photoconductivity to switch connections optically. This simplifies the wiring and also enables non-contact addressability of actuator elements in an array, enabling a greater number of independently controllable degrees of freedom.

Optically addressable dielectric elastomer actuator arrays using embedded percolative networks of zinc oxide nanowires

Ehsan Hajiesmaili*, David R. Clarke
John A. Paulson School of Engineering and Applied Sciences, Harvard University, Cambridge, MA 02138, USA

Dielectric elastomer actuators (DEAs) are electrically driven soft actuators that generate fast and reversible deformations, enabling lightweight actuation of many novel soft robots and haptic devices. However, the high-voltage operation of DEAs combined with the paucity of soft, small high-voltage microelectronics has limited the number of discrete DEAs that can be incorporated into soft robots. This has hindered the versatility as well as complexity of the tasks that they can perform which, in practice, depends on the number of their independently addressable actuating elements. This paper presents a new class of optically addressable dielectric elastomer actuators that utilize the photoconductivity of semiconducting zinc oxide nanowires to create optically switchable and stretchable electrical channels. This enables non-contact, optical control of local actuation. To illustrate the versatility of the new capabilities of this integration, we describe the response of dielectric elastomer actuators with integrated photoconductive channels, formed from thin films of percolating semiconducting nanoparticles. By using a switchable array of small light emitting diodes to optically address the actuator array, its actuation can be controlled both spatially and temporally.

Introduction

Dielectric elastomer actuators (DEAs) [1, 2] are soft capacitors made of thin elastomer layers coated by compliant electrodes. Upon applying voltage, the coulombic attraction of the opposite charges on the compliant electrodes compresses the elastomer layer in thickness, and the incompressibility of the elastomer causes a lateral expansion. These voltage-driven mechanical deformations are fast and reversible and has been used for several novel applications in soft robotics [3-6] and haptics devices [7-10]. The driving voltages of DEA devices are often in the order of several kilovolts and their currents are in the order of tens of micro amperes. The use of high voltages and low currents are inherently neither a drawback nor a safety issue. Rather they result in low ohmic losses, low charging and discharging time constants, and less sensitivity to the impurities such as dust and air bubbles within the elastomer layers and partial coverage of the complaint electrodes for elastomers with larger thicknesses. However, the lack of small, high-voltage, soft microelectronics poses a challenge to addressing of individual actuators in multiple-DEAs arrays and devices. Currently, to address individual actuators, state-of-the-art DEA-based devices mainly use commercially available high-voltage mechanical relays such as 5501-12-1 Coto Relays used in [11], photocell solid-state relays such as AQV258A used in [12], or MOSFETs such as IXTT02N450HV used in [13]. There are, however, two major challenges with even these. First, the volume and weight of these elements can be greater than the actuators themselves and scale up with the number of independently addressable actuators per volume. Second, creating interconnects between large number of addressing elements and actuators increasingly complicates the fabrication process. Significantly, these have limited the number of individually addressable actuators of today's DEA-based devices, limiting the complexity of their attainable functions.

Despite the crucial need for developing integrated high-voltage switches for devices with multiple-DEAs arrays, the reports to date have been of separate switching circuits attached to the DEAs. For instance, Shea's group [14], has described an array of 4×4 high-voltage tin-oxide thin film transistors on a flexible polyimide substrate to control individual DEAs in an array of 4×4 actuators. These operate at voltages larger than 1kV and 20μA current, using gate voltages of 30V, and function even when bent to a 5 mm radius of curvature. High-voltage switches for DEAs were made in [15] by depositing amorphous silicon onto a Kapton foil. The high-voltage switch was then interfaced with

* Corresponding author: hajiesmaili@seas.harvard.edu

a single DEA, allowing for optical addressing of its actuations that were tunable with the light intensities. Similarly, in a more recent study [16], an array of 2×3 photoconductive switches made of amorphous silicon were formed onto a glass substrate and interfaced with an array of DEAs using a set of wires, addressing individual DEAs using patterns of light created by 6 light emitting diodes placed in the vicinity of the photoconductive switches.

In this paper, we introduce fully integrated, embedded high-voltage photoconductive electrical channels for non-contact optical addressing of individual actuators in DEA arrays. These channels are made of percolating networks of photoconductive zinc oxide nanowires formed onto the elastomer layers using the same method as DEAs' stretchable electrodes, providing a simple fabrication of DEA-based devices with multiple actuators and fully integrated photoswitches without any post-fabrication assembling. Percolating networks of zinc oxide nanowires integrated into soft elastomer matrices (or onto elastomer substrates) show low mechanical stiffnesses and high stretchability (13), unlike the zinc oxide nanowires themselves. Although photoconductivity of stretchable electrical channels of percolating networks of semiconducting nanoparticles for optical switching of low-voltage electronics has been studied previously [17], they have not been studied for high-voltage applications or used in any DEA-based devices. However, as will be discussed in the following, these percolating networks of zinc oxide nanowires are particularly suitable for addressing of stretchable DEAs at high operating voltages. In the following, the properties of the percolating channels are first described and then the actuation response when embedded into an elastomer and finally a demonstration of their use in actuating a 6 × 6 DEA array.

Results and Discussions

The physical basis of photoconductive channels consisting of percolating networks of semiconducting nanoparticles is well understood. When illuminated by photons with energies higher than the bandgap, each nanoparticle becomes conductive and, with nanoparticle densities beyond the percolation threshold, networks of electrically conductive paths are formed. The resistance of the network is the sum of the resistance of the nanoparticles, which is tunable by the light intensity, and the contact resistance between the nanoparticles. When the light is removed, the semiconducting nanoparticles, and therefore the percolating network, become insulating again. Zinc oxide nanowires have direct bandgap of 3.3 eV [18], showing photocurrent when illuminated by ultraviolet (UV) light with wavelengths smaller than ~375 nm. The photoconductive response, however, is mainly governed by oxygen adsorption and desorption in air [19-21]. Oxygen atoms chemisorb to zinc oxide nanowire surfaces and act as electron acceptors. When illuminated by UV light, the holes in the photogenerated electron-hole pairs interact with the negatively charged chemisorbed oxygen atoms and make them electrically neutral. These physiosorbed oxygen atoms can leave the surface as a result of thermal vibrations. This process lowers the electron-hole recombination rate, resulting in large numbers of excess electrons in the conduction band, having orders of magnitude higher mobility compared to the holes, and therefore large photocurrents. The photocurrent increases with illumination time until the oxygen adsorption and desorption rates are balanced. As a result, larger photocurrents have been observed at lower oxygen pressures [19]. When the UV light is removed, the limited number of holes limits the electron-hole recombination rate. Instead, oxygen atoms need to be resorbed onto the zinc oxide surfaces to capture the excess electrons and reduce the photocurrent. As a result, slower photocurrent decay rate has been observed at lower oxygen pressures [19]. The process of diffusion of oxygen atoms and resorption onto zinc oxide surfaces is slower than the oxygen desorption caused by interaction of photogenerated holes with charged oxygen atoms, and therefore the photocurrent decay time is slower than the rise time. Both processes are far slower than electron-hole recombination rate, resulting in photocurrent rise and decay times that are in the order of seconds to several minutes [22], as compared to less than a nanosecond for electron-hole recombination. The photocurrent and the rise and decay rates are highly dependent on the environment of zinc oxide nanowires. For this reason, the following presents measurements of photocurrent of percolating networks of zinc oxide nanowires embedded into polyurethane acrylate dielectric elastomers, as functions of time, area density, applied bias voltage, and UV light intensity.

Photocurrent of embedded electrical channels of zinc oxide nanowires

As illustrated in Figure 1(a), to measure photocurrent of percolating networks of zinc oxide nanowires, two islands of percolating networks of carbon nanotubes (CNTs), with dimensions of 10 mm × 10 mm and 1 mm apart from each other, were connected using an electrical channel made of zinc oxide nanowires. The width of the channel is $W = 10$ mm and the length of the channel is $L = 1$ mm and there is 1 mm overlap with each of the two islands of CNTs, shown in gray in Figure 1(a). The CNT electrodes were formed by vacuum filtration of a dispersion of CNTs in deionized water through a porous filter and stamping onto an elastomer substrate, following the procedure described in the appendix of [2]. The elastomer substrate was made of urethane acrylate precursor, spin coated, and cured using ultraviolet light. The percolating network of zinc oxide nanowires were made using the same method as the CNT electrodes; first, zinc oxide nanowires (with diameter of 50 nm to 150 nm and length of 5 μm to 50 μm, SKU: NWZO01A5, ACS Material LLC; Raman spectra shown in Figure S1) were suspended in isopropanol using ultrasonication, followed by vacuum filtration of 4.0 g of the dispersion through a porous filter with 0.2 μm pore sizes, forming percolating networks of zinc oxide nanowires with density of 1.0 g.mm^{-1}. Then, the photoconductive electrical channels were made by stamping the filters onto elastomer substrates. The shape and dimensions of the channel were defined by placing masks between the elastomer and the filter, which were cut from a clear silicone release film. The masks and stamps were then removed, and an encapsulating layer of elastomer was formed on top of the CNT electrodes and zinc oxide channel, using the same material and method as for the substrate. Details of the fabrication method are presented in the supplementary materials.

When a bias voltage of 200 V is applied to the two ends of the CNT islands and the channel illuminated by an array of seven UV light emitting diodes (LEDs) with peak wavelength of 365 nm (ATS2012UV365, Kingbright) and light intensity of 3.41 mW.mm^{-2}, Figure 1(b) at $t = 5$ s, the current through the channel jumped by nearly three orders of magnitude in just a second. This was then followed by a gradual increase over the next nine seconds. When the UV light was removed, Figure 1(b) at $t = 15$ s, the current dropped by one order of magnitude in less than a second and gradually decreased towards zero over tens of seconds.

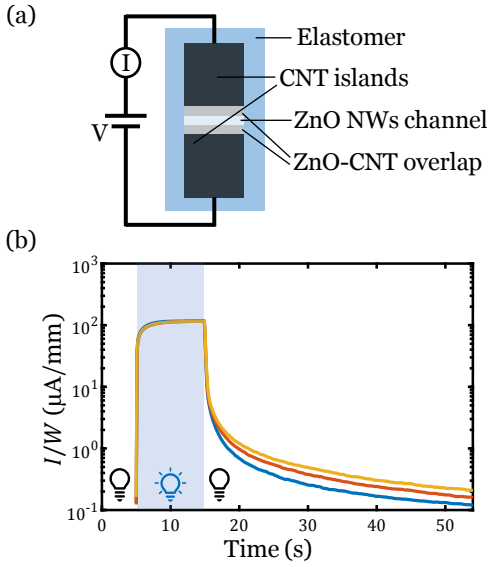

Figure 1. Photocurrent in percolating networks of zinc oxide nanowires. (a) Channels of percolating networks of zinc oxide nanowires were formed onto an elastomer substrate connecting two islands of percolating networks of CNTs, and their photocurrents were measured by applying bias voltages to the two ends of the CNT islands while measuring the current. (b) When the UV light is turned on, at $t = 5$ s, the photocurrent (per width of the channel) jumps by nearly three orders of magnitude followed by a gradual increase while the UV light is on. When the light is turned off, at $t = 15$ s, the photocurrent drops by one order of magnitude in less than one second, followed by a gradual decrease over tens of seconds. Blue, red, and yellow lines show repeatability of runs one to three, respectively.

The photocurrents of the zinc oxide channels are determined by the geometrical dimensions of the channel, density of the zinc oxide nanowires, applied bias voltage, and the incident light. To investigate the effect of each of these parameters on the photocurrent of percolating networks of zinc oxide nanowires, channels with zinc oxide densities of 0.4, 0.6, 1.0, and 2.0 μg.mm^{-2} were fabricated by vacuum filtration and stamping of 1.6, 2.4, 4.0 and 8.0 g of zinc oxide nanowire dispersion, respectively. The photocurrents were measured under bias voltages of 100 and 200 V and UV light intensities of 2.27, 3.41, 4.55, 5.69 mW.mm^{-2}. The measurements and scanning electron microscopy (SEM) images of the percolating networks of zinc oxide nanowires are shown in Figure 2. The conductivities, σ, were calculated from the applied bias voltage, V, measured current, I, and channel dimensions, w and l, as $\sigma = IL/VW$. When UV exposure time is increased from 10s to 100s, transient effects are observed during the first exposure followed by repeatable photocurrents during the following ones, Figure S2. The stability of the zinc oxide nanowires after 10 min UV exposure while the bias voltage is off is shown in Figure S3.

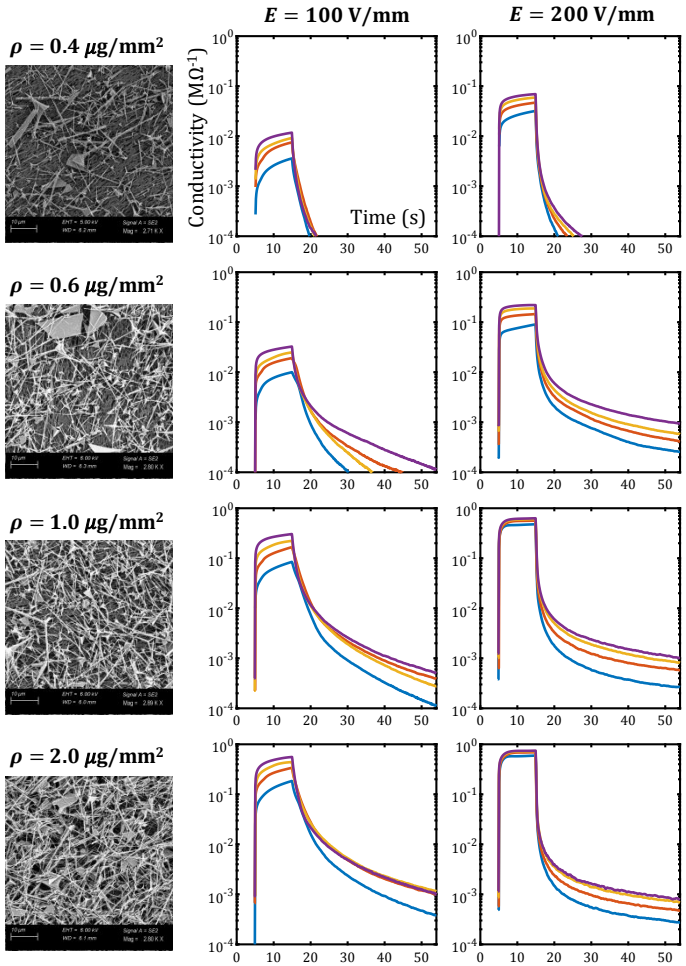

Figure 2. SEM images (first column) and photoconductivity as a function of time at applied bias voltages of 100 and 200 volts (second and third columns, respectively) for channels with zinc oxide nanowire densities of 0.4, 0.6, 1.0, and 2.0 μg.mm^{-2} (rows one to four, respectively), and UV light intensities of 2.27, 3.41, 4.55, 5.69 mW.mm^{-2}, shown with blue, red, yellow, and purple curves, respectively in each graph.

Increasing the density of the zinc oxide nanowires from 0.4 to 1.0 μg.mm^{-2} (rows one to three in Figure 2), increases the photoconductivity, as expected, Figure 3(a). However, the reduction in resistance when the density was increased to 2.0 μg.mm^{-2} was less significant. As seen in the scanning electron microscopy (SEM) images in the left column in Figure 2, at density of 2.0 μg.mm^{-2}, the nanowires started to accumulate on top of each other, shadowing the nanowires underneath and resulting in smaller photocurrent through these shadowed nanowires.

Increasing the applied bias voltage from 100 V to 200 V resulted in higher photoconductivity and faster switching, comparing the dashed and solid lines in Figure 3 (a) and Figure 3 (b), respectively. Therefore, when used to address DEAs that normally operate at few kilovolts, the channels of zinc oxide nanowires are expected to exhibit both faster switching and larger photoconductivity.

Increasing the UV light intensity, reduced the UV-on resistance, as expected, comparing the blue, red, yellow, and purple curves in Figure 3 (a). Therefore, the channels of zinc oxide nanowires not only act as high voltage electrical switches but also tune the voltage drop, controlled by the incident UV light intensity.

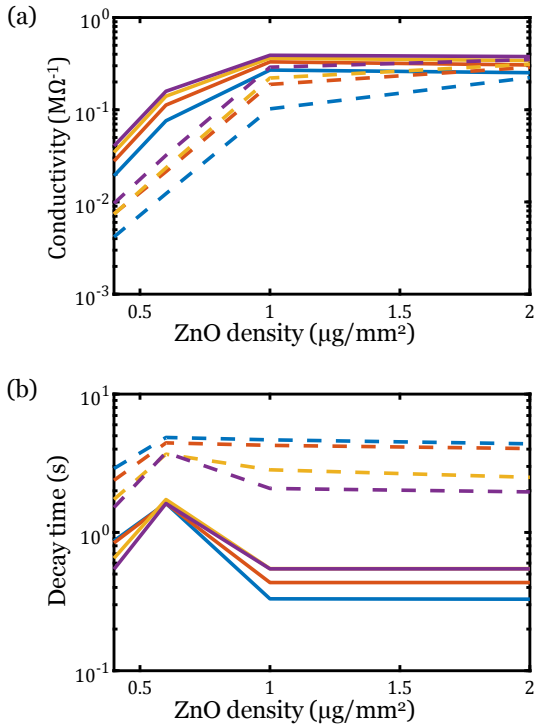

Figure 3. (a) Maximum photoconductivity while the UV light is on and (b) decay time for the conductivity to drop by one order of magnitude when the UV light is turned off, as functions of the zinc oxide nanowires density, under bias voltages of 100 and 200 V, shown with dashed and solid lines, respectively, and UV light intensities of 2.27, 3.41, 4.55, 5.69 mW.mm^{-2}, respectively shown with blue, red, yellow, and purple curves in each graph.

Electrical breakdown strength of channels of zinc oxide nanowires

When used to address DEAs, channels of zinc oxide nanowires need to withstand large bias voltages and allow minimal leakage currents when there is no UV illumination. For this reason, leakage current and electrical breakdown strength of channels of zinc oxide nanowires with densities of 0.4, 0.6, 1.0, and 2.0 μg.mm^{-2}, were measured at the absence of UV light, shown in Figure 4. The zinc oxide channel showed no measurable current until the applied voltage reached ~6 kV, at which electrical breakdown occurred along the zinc oxide channel, indicated by a jump in current shown in Figure 4(a), and physical damage to the channel shown in Figure 4(b). No correlation between the electrical breakdown strength and the density of zinc oxide nanowires were found, and the leakage current remained below the minimum measurable current of 0.06 μA for all four channels until breakdown. The high electrical breakdown strength of 6 kV per mm of the channels' length, even when high densities of zinc oxide nanowires are used, is particularly important for addressing DEAs that normally operate at a few kilovolts. Indeed, it is expected that the electrical breakdown of the percolating network of zinc oxide nanowires will limit the minimum length of the channel and the size scaling of the devices. For instance, for a DEA device operating at 3 kV, the channel needs to be at least 0.5 mm long to below the breakdown condition.

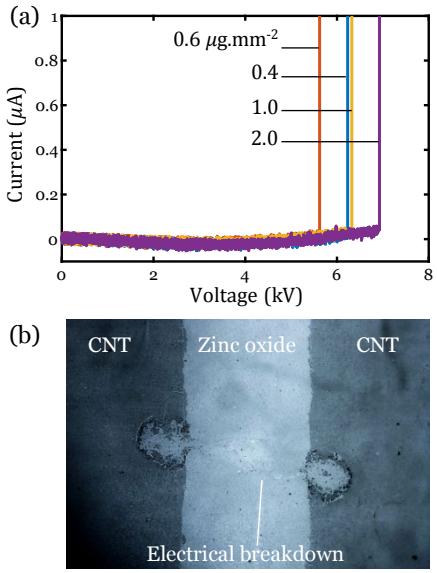

Figure 4. Electrical breakdown of channels of percolating networks of zinc oxide nanowires. (a) Channels with zinc oxide nanowire densities of 0.4-2.0 μg.mm^{-2} show no measurable current at the absence of the UV light, until a sudden jump in current occurs because of electrical breakdown at ~6 kV.mm^{-1} (No clear correlation with the zinc oxide nanowire density is evident). (b) Optical microscope image of the electrical breakdown path through the zinc oxide channel with density of 0.6 μg.mm^{-2}. Note, the crater - like damage produced by the electrical breakdown.

Actuation time response of DEAs with embedded zinc oxide nanowires channels

To characterize actuations of DEAs addressed by zinc oxide nanowire channels, the arrangement shown in Figure 5(a) was prepared. The actuator consisted of multiple elastomer layers, shown in translucent grey in Figure 5(a), high voltage electrodes, shown in red, and ground electrodes, shown in blue. The actuator had ten active elastomer layers elastomer, 25 mm in diameter and 0.6 mm in total thickness, with eleven interdigitated high-voltage and ground CNT electrodes, only one of each is shown in Figure 5(a) for simplicity. Details of the fabrication methods of the elastomer layers and CNT electrodes are presented in the Supplementary Materials. To simplify the actuation measurements, the DEA was mounted onto a circular frame, shown in green in Figure 5(a), forcing the DEA to move out of the plane, and the out-of-plane displacement was measured using a laser line scanner (MTI ProTrak, PT-G 60-40-58). The ground electrode of the DEA was connected to the ground terminal of the power supply (Trek 610E, Advanced Energy) and the high voltage electrode of the DEA was either connected to the high voltage (1.5 kV) or ground terminal of the power supply using either a set of zinc oxide nanowires channels with 1.0 μg.mm^{-2} density or photocell solid-state relays (AQV258A, Panasonic), the latter serving as the ideal switching response with negligible leakage current and response time compared to the DEA.

When the solid-state relay 1, in Figure 5(a), connected the high-voltage electrode of the DEA to the high-voltage terminal of the power supply, the DEA buckled out of plane in less than 100 ms after the in-plane stress reached the threshold for out-of-plane buckling in less than 40 ms. The time response of the out-of-plane actuation, Z, is shown with black curves in Figure 5(b). The out-of-plane buckling in the downward direction (negative Z) was restricted using a stiff block placed about 0.5 mm below the actuator. When solid-state relay 1 was turned off and relay 2 was turned on, connecting the high-voltage electrode of the DEA to the ground terminal of the power supply, the actuator moved back to its original flat configuration, but with slower time response as compared to the actuation rate: the out-of-plane deformation retracted by about 0.7 mm, 50 ms after solid-state relay 2 was turned on, compared with the actuation of 2.5 mm, 50 ms after its out-of-plane buckling threshold was reached when solid-state relay 1 was turned on.

To address the DEA using zinc oxide nanowires channels, channel 1 in Figure 5(a) was illuminated using two UV LEDs placed onto the channel, connecting the high-voltage electrode of the DEA to the high-voltage terminal of the power supply. To remove the actuation, the UV illumination of channel 1 was turned off and the zinc oxide channel

2 was illuminated with two UV LEDs, connecting the high-voltage electrode of the DEA to the ground terminal of the power supply. Out-of-plane actuation time response of the DEA when addressed using zinc oxide nanowire channels are shown with red, purple, cyan, and blue curves in Figure 5(b) for illuminated UV light intensities of 2.27, 3.41, 4.55, 5.69 $mW.mm^{-2}$, respectively. Significantly, the time required to reach the threshold for out-of-plane buckling was higher with the zinc oxide nanowires channels, compared to that of solid-state relays, but reduced with increasing the light intensity, ranging from 130 ms for 2.27 $mW.mm^{-2}$ to 60 ms for 5.69 $mW.mm^{-2}$. The actuation magnitude of the DEA increased marginally with the light intensity, ranging from 2.22 for 2.27 $mW.mm^{-2}$ to 2.37 mm for 5.69 $mW.mm^{-2}$, compared to ~2.8 mm when actuated using solid-state relays, i.e. 15% to 21% less. When channel 2 was illuminated and the channel 1 was turned off, the higher light intensity also resulted in faster time response: 100 ms after the channel 2 is turned on, the actuation dropped to 1.1 to 1.5 mm for light intensities of 2.27 to 5.69 $mW.mm^{-2}$, respectively, far from 0.5 mm for solid-state relay. However, after 500 ms the difference reduces to less than 0.1 mm. These confirm that embedded percolating networks of zinc oxide nanowires can be used as integrated high-voltage switches for non-contact optical addressing of DEAs, however with some limitations: at 1Hz, the actuation displacement reduces by %15~%20 and decreases further with the actuation frequency.

The cycling tests of the DEA when addressed using the solid-state relays and zinc oxide channels with illuminated UV light intensity of 2.27 $mW.mm^{-2}$ are plotted in black and red in Figure 5(c), respectively, showing that when actuated for 1000 cycles, the actuation magnitudes and response times for the first and last ten cycles are similar, presented in the left and right panels, respectively. This confirms robust performance of DEAs with zinc oxide nanowires over large numbers of cycles. Real-time cyclic actuation of the DEA using the zinc oxide nanowires channels and photocell solid-state relays is shown in Supplementary Movie S1.

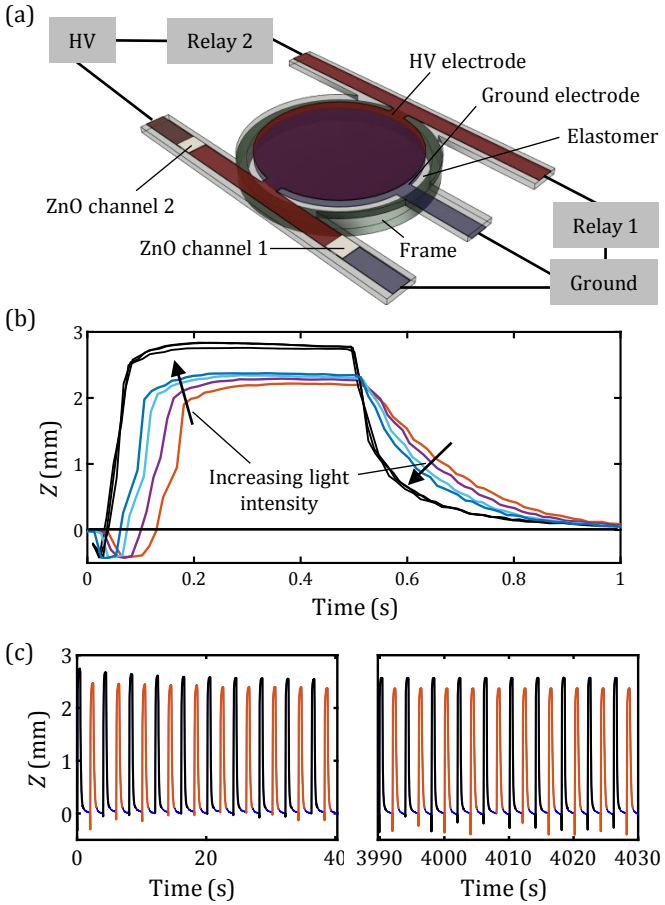

Figure 5. Actuation of a multilayer DEA with zinc oxide nanowire channels. (a) The actuator consists of a ground electrode, shown in blue, a high voltage (HV) electrode shown in red, and an elastomer layer shown in translucent gray, mounted onto a rigid ring, shown in green. The actuator consisted of ten active layers, only one layer of which is shown in this schematic for simplicity. The

HV electrode is either connected to the high-voltage or ground terminal of the power supply, addressed by either two zinc oxide nanowire channels or two solid-state relays, enabling the time responses to be compared. (b) Time response of the DEA at 1Hz using solid-state relays, shown with black lines, and using zinc oxide channels and light intensities of 2.27, 3.41, 4.55, 5.69 $mW.mm^{-2}$, shown in red, purple, cyan, and blue, respectively. (c) First and last ten actuation cycles of the DEA, shown in the left and the right panels, respectively, when actuated for 1000 cycles alternating between the solid-state relays and zinc oxide nanowire channels, shown in black and red respectively.

Addressing arrays of DEAs using integrated channels of zinc oxide nanowires

As an example of the new design space enabled by integrating percolating networks of zinc oxide nanowires into DEAs, local actuations of a sheet of DEAs, optically addressed using channels of zinc oxide nanowires, are demonstrated in Figure 6. The device consists of two elastomer layers fabricated separately and attached together: one layer is an elastomer sheet with an array of DEAs that produce mechanical actuations, Figure 6(a), and the other is an elastomer sheet with embedded UV LEDs that are attached to a Bluetooth low energy (BLE) module and optically addresses the zinc oxide channels and control the actuation of DEAs, Figure 6(b).

The multilayer 6×6 array of DEAs, Figure 6(a), was created by a sequence of, first, spin coating and UV curing of CN9028 elastomer, and second, forming arrays of 6 rectangular CNT electrodes onto the elastomer layer, oriented perpendicular to the electrode arrays on the adjacent layers. Concentric square-shaped rings were printed onto each individual DEA to create larger out-of-plane deformations, following the methods described in [23]. The 6×6 array of DEAs was connected to high voltage and ground terminals of a miniature power supply (EMCO Q50-5, XP Power) through two sets of 6 channels of percolating zinc oxide nanowires with area density of 1.0 $\mu g.mm^{-2}$. The channels were formed by vacuum filtration and stamping of zinc oxide nanowires, the same method used to form the CNT electrodes, simplifying the integration of the high-voltage switches of zinc oxide nanowires. Interdigitated electrodes were connected to each other using vias made by cutting holes through the elastomer layers and CNT electros and filling with carbon conductive grease (8481-1, MG Chemicals), indicated in the inset in Figure 6(a).

Separately, as shown in Figure 6(b), two sets of UV LEDs (ATS2012UV365, Kingbright) were embedded into an elastomer sheet and connected to a BLE module (CYBLE-212006-01, Cypress Semiconductor) using thin shielded copper wires. The LEDs were positioned such that when the two elastomer sheets shown in Figure 6 (a) and (b) were attached together, each LED was placed above a zinc oxide channel, as show in Figure 6(c). The LEDs are controlled using a smartphone app developed to connect to the BLE module. The smartphone app and BLE module program are provided as Supplementary Materials. Both the BLE module and the power supply were powered by a 3.7 V battery with 1000 mAh capacity (DTP 603450).

To address an individual DEA in the 6 x 6 array, one pair of the LEDs are turned on, activating a pair of zinc oxide nanowire channels, connecting the DEA to the high voltage and ground terminals of the power supply. Figure 6(d, e) show examples of actuations of two individual DEAs, recorded from a video of the actuations (Supplementary Materials. Both real-time actuation of the entire device, and a magnified view of the actuators array at 4x speed are shown). The changes are seen most vividly in the video which also illustrate that the actuator response is significantly slower than the photoconductive responses shown in figure 2 and 5. This difference is attributed to the small current that the onboard power supply and battery provide and the small leakage current of the elastomer, contributing to the slower actuation and removal of actuation, respectively. Further improvements in the DEA array are expected to result in time response matching that of the DEA shown in Figure 5.

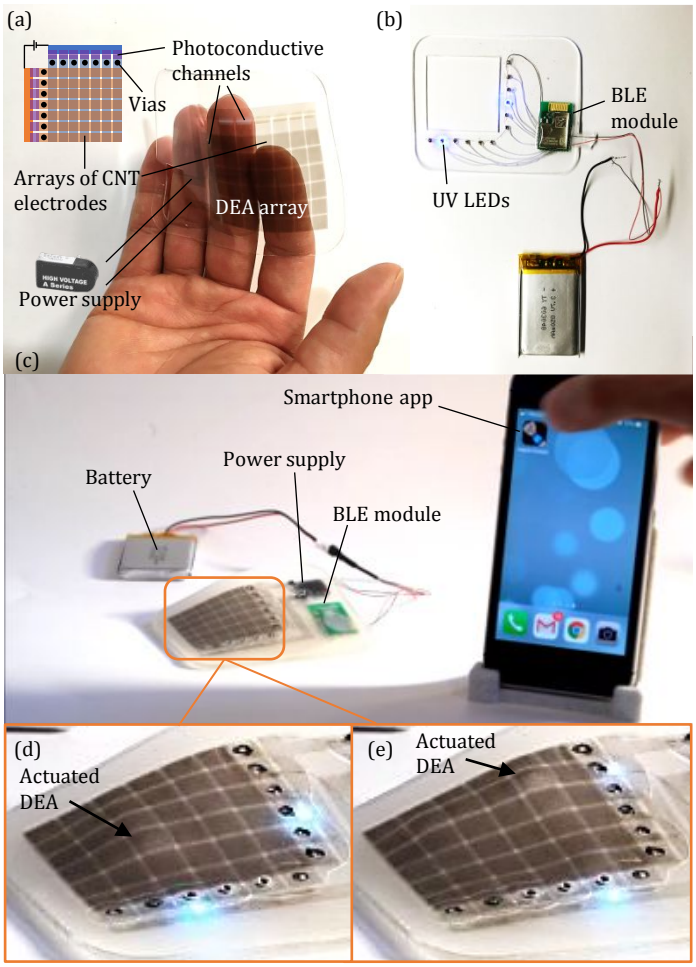

Figure 6. An example of an optically addressable DEA array with integrated channels of zinc oxide nanowires. (a) An array of 6×6 multilayer DEAs were fabricated and connected to the positive and negative terminals of a power supply through two sets of 6 channels of zinc oxide nanowires. (b) Two sets of 6 UV LEDS were embedded into an elastomer sheet and connected to a BLE module using shielded copper wires. (c) The two layers in (a) and (b) were attached to each other and the BLE module and power supply were connected to a 3.7 V battery. A smartphone app was developed to connect to the BLE module and control switching of pairs of UV LEDs. (d, e) Two examples of addressing individual DEAs when pairs of UV LEDs are turned on (shining blue).

Conclusions

The characterizations shown in Figures 2-5 confirm that the integrated zinc oxide nanowire networks are particularly well-suited for non-contact optical addressing of DEAs. They show an order of magnitude increase in photoconductivity in a fraction of second (and nearly three orders of magnitude in just a second) when exposed to the UV light and a decay time of nearly one second when the UV light is removed, which match the typical 1 Hz operating frequency of DEA-based devices. Their electrical breakdown strength of 6 kV per mm of channel length is enough for withstanding DEAs' typical operating voltages of less than 3 kV using channels with 0.5 mm length. Their mechanical compliance [17] and their simple fabrication method that follows the same process as for the compliant electrodes allows for their full integration into DEAs' electrodes to address local actuations of DEA-based devices with high spatial resolutions, without any post-fabrication assembling and interfacing.

Although channels of zinc oxide nanowires activated by only a few UV LEDs have been described in this paper, the integration of percolating networks of zinc oxide nanowires into DEA devices enables a larger design space for novel DEA-based devices. For instance, percolating networks of zinc oxide nanowires can replace CNT electrodes and serve as locally addressable electrodes, activated remotely by projected patterns of UV lights. When combined with high-resolution optical displays and projectors, percolating networks of zinc oxide nanowires can facilitate actuations with high spatial resolutions. Additionally, integrated percolating networks of semiconducting nanoparticles other than zinc oxide nanowires can be used that respond to other or multiple light wavelengths, e.g., percolating networks

of cadmium sulfide nanoparticles with direct bandgap of 2.42 eV can be used and activated by visible light with wavelengths up to 550 nm.

In summary, integration of percolating networks of zinc oxide nanowires into DEAs, operating at high voltages, allows for optical addressing of individual actuators in a noncontact manner using common low-voltage electronics. It was shown that channels of zinc oxide nanowires can withstand high operating voltages of DEAs in the absence of UV light and exhibit fast response and large photocurrent to dark current ratio under high bias voltages. Finally, optical addressing of a 6×6 array of DEAs with integrated channels of zinc oxide nanowires was demonstrated as an example.

Acknowledgement

The authors are grateful to Dr. Alex Chortos, now at Purdue University, for assistance in fabricating the arrays, to Dr. Matthias Kollosche for the SEM images in Figure 2, and to Victor Champaign for measuring the Raman spectra of the zinc oxide nanowires.

Funding: This work was supported by the National Science Foundation through the Harvard University Materials Research Science and Engineering Center DMR-2011754.

Competing interests: The authors declare that they have no competing interests.

Data and materials availability: All data needed to evaluate the conclusions in the paper are present in the paper and/or the Supplementary Materials.

References and Notes

1. Pelrine, R., et al., *High-speed electrically actuated elastomers with strain greater than 100%.* Science, 2000. **287**(5454): p. 836-839.
2. Hajiesmaili, E. and D.R. Clarke, *Dielectric elastomer actuators.* Journal of Applied Physics, 2021. **129**(15): p. 151102.
3. Duduta, M., D.R. Clarke, and R.J. Wood. *A high speed soft robot based on dielectric elastomer actuators*. in *2017 IEEE International Conference on Robotics and Automation (ICRA)*. 2017. IEEE.
4. Gu, G., et al., *Soft wall-climbing robots.* Science Robotics, 2018. **3**(25).
5. Chen, Y., et al., *Controlled flight of a microrobot powered by soft artificial muscles.* Nature, 2019. **575**(7782): p. 324-329.
6. Li, G., et al., *Self-powered soft robot in the Mariana Trench.* Nature, 2021. **591**(7848): p. 66-71.
7. Zhao, H., et al., *A wearable soft haptic communicator based on dielectric elastomer actuators.* Soft robotics, 2020. **7**(4): p. 451-461.
8. Matysek, M., et al. *Dielectric elastomer actuators for tactile displays*. in *World Haptics 2009-Third Joint EuroHaptics conference and Symposium on Haptic Interfaces for Virtual Environment and Teleoperator Systems*. 2009. IEEE.
9. Lee, H.S., et al., *Design analysis and fabrication of arrayed tactile display based on dielectric elastomer actuator.* Sensors and Actuators A: Physical, 2014. **205**: p. 191-198.
10. Mun, S., et al., *Electro-active polymer based soft tactile interface for wearable devices.* IEEE transactions on haptics, 2018. **11**(1): p. 15-21.
11. Chortos, A., et al., *Printing reconfigurable bundles of dielectric elastomer fibers.* Advanced Functional Materials, 2021. **31**(22): p. 2010643.
12. Hajiesmaili, E. and D.R. Clarke, *Crosstalk issues in addressing arrays of dielectric elastomer actuators*, in *EuroEAP 2021*. 2021.
13. Hajiesmaili, E., *Shape-Morphing Dielectric Elastomer Devices*, in *Graduate School of Arts and Sciences*. 2022, Harvard University.
14. Marette, A., et al., *Flexible zinc–tin oxide thin film transistors operating at 1 kV for integrated switching of dielectric elastomer actuators arrays.* Advanced materials, 2017. **29**(30): p. 1700880.
15. Lacour, S.P., et al., *Mechatronic system of dielectric elastomer actuators addressed by thin film photoconductors on plastic.* Sensors and Actuators A: Physical, 2004. **111**(2-3): p. 288-292.

16. Bacheva, V., et al. *Photoconductive Switching of a High-Voltage Actuator Array*. in *2022 IEEE 35th International Conference on Micro Electro Mechanical Systems Conference (MEMS)*. 2022. IEEE.
17. Yan, C., et al., *An intrinsically stretchable nanowire photodetector with a fully embedded structure.* Advanced Materials, 2014. **26**(6): p. 943-950.
18. Srikant, V. and D.R. Clarke, *On the optical band gap of zinc oxide.* Journal of Applied Physics, 1998. **83**(10): p. 5447-5451.
19. Melnick, D.A., *Zinc oxide photoconduction, an oxygen adsorption process.* The Journal of Chemical Physics, 1957. **26**(5): p. 1136-1146.
20. Collins, R. and D. Thomas, *Photoconduction and surface effects with zinc oxide crystals.* Physical Review, 1958. **112**(2): p. 388.
21. Li, Q., et al., *Adsorption and desorption of oxygen probed from ZnO nanowire films by photocurrent measurements.* Applied Physics Letters, 2005. **86**(12): p. 123117.
22. Chang, S.-P. and K.-J. Chen, *Zinc oxide nanoparticle photodetector.* Journal of Nanomaterials, 2012. **2012**.
23. Hajiesmaili, E., et al., *Voltage-controlled morphing of dielectric elastomer circular sheets into conical surfaces.* Extreme Mechanics Letters, 2019. **30**: p. 100504.